Thin adhesive oil films lead to anomalously stable mixtures of water in oil

Claire Nannette, Jean Baudry, Anqi Chen, Yiqiao Song, Abdulwahed Shglabow, Nicolas Bremond, Damien Démoulin, Jamie Walters, David Weitz, Jérôme Bibette

Title:

Thin adhesive oil films lead to anomalously stable mixtures of water in oil

Authors: Claire Nannette[1,2], Jean Baudry[1], Anqi Chen[3], Yiqiao Song[3,6], Abdulwahed Shglabow[1], Nicolas Bremond[1], Damien Démoulin[2], Jamie Walters[2], David A. Weitz[3,4,5], Jérôme Bibette[1]*

Affiliations:
[1]Laboratoire Colloïdes et Matériaux Divisés, CBI, ESPCI Paris, Université PSL, CNRS; Paris, 75005, France
[2]Calyxia; Bonneuil-sur-Marne, 94380, France
[3]John A. Paulson School of Engineering and Applied Sciences, Harvard University; Cambridge, MA 02138, USA
[4]Department of Physics, Harvard University; Cambridge, MA 02138, USA
[5]Wyss Institute for Biologically Inspired Engineering, Harvard University; Boston, MA 02215, USA
[6]Athinoula A. Martinos Center for Biomedical Imaging, Department of Radiology, Massachusetts General Hospital; Charlestown, MA 02129, USA
*Corresponding author. Email: jerome.bibette@espci.fr

Abstract:

Oil and water can only be mixed by making droplets of one fluid in the other. When two droplets approach one another, the thin film that separates them invariably becomes unstable, causing the droplets to coalesce. The only known way to avoid this instability is through addition of a third component, typically a surfactant, which stabilizes the thin film at its equilibrium thickness. We report the observation that a thin fluid film of oil separating two water droplets can lead to an adhesive interaction between the droplets. Moreover, this interaction prevents their coalescence over time scales of several weeks, without the use of any surfactant or solvent.

One-Sentence Summary: Adsorption of polymeric oil on a water interface leads to weak adhesion and metastability for emulsion droplets

Main Text:

Oil and water do not mix. When the two are violently shaken together, droplets of one fluid will form inside the other, but when two droplets are brought in close proximity to one another they are unstable and coalesce to form a single droplet. As the interfaces approach one another, the intervening fluid layer becomes very thin and thermally induced capillary waves on each interface lead to merging (*1*). This can only be avoided through the addition of a third component, a surfactant, which induces a repulsive interaction that prevents spontaneous coalescence due to capillary waves, except in highly specific cases such as water-in-liquid-crystal emulsions (*2*), some very dilute charged systems (*3*) or when some intrinsic impurities can act as surfactant (*4*). Instead, coalescence can only occur in the thin fluid film separating the droplets through a thermally activated nucleation of a hole that must reach a critical size above which it becomes unstable (*5*). The activation energy for nucleation of a hole can be large, leading to long term stability of the surfactant stabilized droplets. In some cases there can be an attractive interaction which causes droplets to adhere to one another while still retaining their integrity due to the adsorbed surfactant (*6*). For example, a classic observation is when oil droplets in water, commonly called direct emulsions, are stabilized by a widely used surfactant such as SDS (sodium dodecyl sulfate). The addition of excess salt causes interfaces of neighboring droplets to wet one another resulting in a very thin water film separating the

droplets (*7*). This leads to adhesion but the stability of the droplets is retained. Similar behavior can be observed for water droplets in oils, commonly called inverse emulsions: Addition of a solvent to the oil can cause the surfactant stabilizing the droplets to become less soluble in the continuous phase, and hence induce an attractive interaction which leads the droplets to wet one another; nevertheless coalescence is still avoided due to the surfactant (*8*, *9*). Attractive interactions between droplets can only occur when molecules at the interface of the droplets are more compatible with one another than with the solvent itself. In all cases stability of a thin oil film separating two water droplets can only be achieved through the incorporation of one or more additional components able to adsorb at the interfaces (*10*).

We report the spontaneous formation of an anomalously stable thin film of oil between droplets of water for a polymeric oil. When there is weak adsorption of the oil on the water interface, the oil molecules at the interface become less compatible with the bulk oil, resulting in a weak attractive interaction between the two water droplets which induces a dramatic change in the dynamics of the oil molecules within the thin film. As a result, the water droplets can remain stable over large time scales, even in the absence of surfactant or any other additional components whatsoever. By measuring the temperature dependence of this stability, we show that it results from an increase, by seven orders of magnitude, in the effective viscosity of the oil in the thin adhesive films between the droplets, as compared to the bulk viscosity. As a consequence, stable water-in-oil emulsions can be produced in the absence of surfactant even at very high volume fractions of water. Moreover, because of this unexpected metastability, above a characteristic water volume fraction, ϕ^*, the emulsion breaks under shear and spontaneously forms double emulsion globules comprised of the primary water-in-oil dispersion.

Adhesion of stable oil films separating water interfaces.

To illustrate this phenomenology, we investigate the behavior of a pure binary mixture of glycerol and polydimethylsiloxane (PDMS) (**fig S1**). We mix glycerol ($\eta_g = 0.84$ Pa. s) into PDMS oil ($M_w = 30\,000$ g/mol) (*11*) with a viscosity of $\eta_0 = 1$ Pa. s to form glycerol droplets of diameter D of about 2 μm (Methods 1). As the droplets approach one another, instead of coalescing, they stick to each other while still retaining their integrity (**Fig 1A**). The existence of these compact clusters indicates that there must be an adhesive interaction between droplets. To confirm this, we use micropipette aspiration to immobilize a doublet comprised of one droplet adhering to a second (Methods 2). The two droplets adhere to one another, demonstrating the attractive interaction, as shown in **Fig. 1B**. To measure this attractive interaction, we illuminate the interface between two droplets with a laser and analyze the resultant interference pattern (*12*). The adhesive patch causes a black central circle in the interference pattern, as seen in **Fig. 1C**. The size of this circle enables us to determine the diameter of the adhesive patch (*7*), a, from which we deduce the contact angle of the adhesive droplets, θ , which we find to be $\theta = 2°$ (Methods 3 and **S**) (*13*). By determining the surface tension between glycerol and PDMS, $\gamma = 25$ mJ/m^2, we can determine the adhesive energy (*14*), $\varepsilon = 2\gamma(1 - \cos\theta)$, which gives $\varepsilon = 3 \times 10^{-2}$ mJ/m^2. For two identical droplets, if $\varepsilon/\gamma \ll 1$, the diameter of the adhesive patch must scale with the diameter of the drop as (*6*) $\left(a/D\right)^2 = \varepsilon/\gamma$. Although the area of each adhesive patch is very small, coalescence must take place within the patches since the contact angle leads to further separation of neighboring interfaces.

Origin of the stability of the thin oil films

To quantify the stability of these thin adhesive oil films, we measure the time evolution of the size distribution of droplets due to coalescence which is the dominant mechanism of coarsening (**movie S1**). We use an emulsion with a volume fraction, $\phi = 76\%$, which is high enough to preclude any significant relative motion of the droplets, ensuring that the measured coalescence rate reflects only the intrinsic instability of the thin films separating droplets in contact with one another (*15*). We determine the number-averaged size distribution (Methods 4). It maintains a constant shape while the mean size increases with time, as shown in **Fig. 2A.** To probe the nature of the metastability of the thin oil film, we measure the temperature dependence of the evolution of the mean diameter: For each temperature, T, the initial time dependence of D is linear, while the rate of growth increases markedly with increasing T, as shown in **Fig. 2B.** The frequency of coalescence, ω, is proportional to the rate of growth normalized by the initial drop diameter. We find that log ω depends linearly on the inverse of T, as shown in **Fig. 2C**. Thus, the coarsening exhibits an Arrhenius behavior given by $\omega = \omega_0 e^{-E_a/k_B T}$, where ω_0 is the attempt frequency, k_B is Boltzmann's constant, and E_a is the energy barrier for the nucleation of a hole, of critical radius, r^*, in the thin film separating two droplets, which induces coalescence. From the slope of the data, we determine $E_a = 20\, k_B T$, with $T = 298$ K. By comparison, surfactant stabilized emulsions typically exhibit a significantly higher energy barrier of at least $30\, k_B T$ (*16*).

To determine the value of r*, we use the simplest model of nucleation and growth, the capillary model (*17*). The energy, $E(r)$, of a hole of radius, r, is $E(r) = -2\pi r^2\gamma + 2\pi r\Gamma$, where γ is the surface tension and Γ is the line tension which accounts for all contributions associated with the inherent high curvature along the perimeter of the hole (**S**). This leads to $r^* = \left(\frac{E_a}{2\pi\gamma}\right)^{1/2}$, and we obtain $2r^* = 1.4$ nm. From this value, we can also infer the thickness of the film, h, which, as assumed by the capillary model, must be of the same order of magnitude, a few nm (*18*).

Further insight into the nature of this behavior comes from determining the attempt frequency, $\omega_0 \sim 10^5$ s^{-1}, which is obtained from the intercept of the fit to the data in **Fig. 2C**. The nucleation rate of a hole (*19*), k_0, is determined by a balance between surface tension, which drives the growth of the hole, and the viscosity of the oil in the film, which slows the growth, $k_0 \sim \frac{\gamma}{\eta r^*}$. The value of ω_0 is determined by k_0 normalized by the number of holes possible, $\omega_0 = k_0 \frac{s}{r^{*2}}$, where *s* is the specific surface area of one drop in contact with its neighboring droplets, where coalescence must occur. Each drop is surrounded on average by a number, z, of neighboring droplets. Therefore, the fraction of the drop surface occupied by adhesive patches is $z\left(a/D\right)^2$, which is about 1% of the drop surface if we assume $z = 10$, as expected for a densely packed emulsion. Thus, within the thin adhesive film, the effective viscosity of the oil, η_{eff}, must be a factor of $\sim 10^7$ more than η_0 (**fig. S2**). It is this large increase in the viscosity in the thin film where coalescence takes place that compensates for the relatively low activation energy and leads to this stable thin adhesive film. The uncertainty of this estimate is about an order of magnitude, given the uncertainty in the determination of ω_0 and k_0.

Molecular nature of the thin oil films

We must therefore consider the nature of this thin adhesive film more carefully. A PDMS molecule at a hydrophilic interface spreads and forms a nm-thick layer (*20*, *21*). The preferential adsorption of the oxygen along the PDMS backbone leads to an excess of hydrophilicity at the glycerol interface; this must be compensated by an excess of hydrophobicity localized on the opposite side, as shown schematically in **Fig. 3A**. Thus, two identical mirror-image layers will weakly adhere to one another instead of remaining surrounded by bulk oil molecules. For a glycerol-PDMS interface in contact with its mirror-image, the whole film tension is lowered by $\varepsilon/2$, which is much smaller than γ. While this energy is relatively small, we hypothesize that it nevertheless creates patches within which the molecular dynamics are severely impacted leading to the very large increase in effective viscosity. Van der Waals interactions could also contribute to the adhesion energy that we measure, however the persistence of the thin adhesive film reflects the existence of a short range repulsion which must be set solely by an interplay between chain adsorption and adhesion of hydrophobic moieties (**S**). Moreover, because this mechanism is molecular in scale, the thickness of these thin films must also be molecular in scale in agreement with measurement on a single interface, and in accord with the value deduced by the capillary model (*17*, *18*).

To explore the molecular basis of this hypothesis, we perform Nuclear Magnetic Resonance (^{1}H NMR) measurements on concentrated glycerol-PDMS emulsions with ϕ between 60% and 76% (Methods 5). We focus on the spin-spin relaxation time (T_2) of the PDMS, which reflects its molecular motion (*22*). For the most concentrated emulsion, $\phi = 76\%$, we observe a pronounced peak, P_1, in the T_2 relaxation time distribution centered around 9×10^{-3} s, which is a factor of 14 less than the peak, P_0, for the same PDMS in the absence of any glycerol. There is, in addition, a second peak, P_2, which appears as a shoulder around 5×10^{-2} s, as shown in **Fig. 3B**. When the volume fraction is decreased to $\phi = 60\%$, P_1 has a smaller amplitude but remains at nearly the same position, while P_2 becomes more pronounced and shifts towards P_0, as shown in **Fig. 3B**.

To account for these NMR results, we hypothesize that there are two types of PDMS molecules within the concentrated emulsion: one type has slow dynamics, and thus short T_2, which is nearly independent of ϕ, as shown by the position of P_1, which remains approximately constant as ϕ changes. The other type has faster dynamics and thus longer T_2, but does change with ϕ. We hypothesize that the first type represents PDMS molecules that are located in the direct vicinity of the thin adhesive film separating droplets, while the second type represents PDMS molecules that are located in the Plateau borders and includes both the molecules within the pore and those adsorbed on the pore surface but not in direct vicinity of the adhesive patches, as depicted in **Fig. 3C**. Since the average dynamics of molecules within a pore includes contributions from both the oil molecules adsorbed on the glycerol interface, and the oil molecules confined within the pore, the peak position should change with ϕ as the relative amount of PDMS adsorbed to the interface changes as the pore size changes; this is indeed what we observe for P_2, consistent with our hypothesis. By contrast, the dynamics of the PDMS molecules in the vicinity of the thin adhesive film includes contributions from those molecules confined within adhesive patch itself and some molecules in close proximity to it. The structure and size of these thin films are preserved by the adhesive forces, independent of dilution. Therefore, the position of the P_1 peak, which is associated with them, should not change with ϕ. However, its amplitude should decay since the proportion of thin films decreases as ϕ decreases. This is indeed what we observe for P_1, consistent with our hypothesis (**S**). For the highest volume fraction, $\phi = 76\%$, the T_2 value of P_1 corresponds to an effective viscosity (*23*) $\eta_{\text{eff}} \approx 10^4\, \eta_0$; this must reflect contributions of the strongly adhesive

molecules directly in the film itself and the neighboring molecules whose motion is restricted but not as strongly. Thus, these molecular-scale NMR results exhibit a trend that is consistent with the large increase in η_{eff} determined from the analysis of the hole nucleation attempt frequency.

Evidence of a generic metastability mechanism

The observation of stable oil films extends beyond this PDMS oil. We produce emulsions with several different oils and hydrophilic phases; each emulsion remains stable. For the aqueous phase we use either glycerol or water with the addition of a few percent sodium alginate to match the oil viscosity to optimize emulsification. For each combination, we measure the characteristic water volume fraction, at which the emulsion breaks under shear and spontaneously forms double emulsion globules comprised of the primary water-in-oil dispersion. This provides a convenient comparison among different fluid pairs. In all cases, ϕ^* depends only on the specific choice of the fluids, and not on how they are mixed. Moreover, in all cases, after dilution, we observe clusters reflecting an attractive interaction between the droplets.

We first compare the behavior of hydroxy-terminated PDMS of the same molecular weight to that of the methyl-terminated PDMS oil. Although this is a very slight modification in the molecular structure, which corresponds to the replacement of only two methyl groups out of approximately 600, it nevertheless induces a large change in ϕ^*: highly-packed emulsions remain stable at even higher volume fractions, up to $\phi^* = 95\%$, as shown in **Fig. 4A.** Upon dilution, we observe the presence of large and dense clusters, which reflects an even stronger adhesive interaction, as seen in **Fig. 4B**. Above ϕ^* the emulsion breaks under shear into a double emulsion comprised of globules with an internal glycerol volume fraction $\phi_{\text{int}} = 86\%$ (Methods 6), and with somewhat larger water droplets, as shown in **Fig. 4C**. We also make stable emulsions using acrylated vegetable oils; a fluorescent image of such an emulsion with $\phi = 70\%$ is shown in **Fig. 4D.** By contrast to the PDMS oils, these emulsions have a lower $\phi^* = 71\%$. Upon dilution, we observe much smaller clusters reflecting a weaker adhesive interaction between interfaces, as seen in **Fig. 4E.** Above ϕ^*, the emulsion breaks into a double emulsion comprised of globules with significantly larger water droplets, as shown in **Fig. 4F.** This acrylated oil has a polymeric backbone **(fig. S3)** which should lead to weaker adsorption and hence lower adhesion, consistent with the smaller clusters observed upon dilution. We summarize the values of ϕ^* and ϕ_{int}, for PDMS, hydroxy PDMS, acrylated vegetable oil and polyester oil in **Fig. 4G**. Further exploration of which oils make stable inverse emulsions with either pure water, water with sodium alginate or glycerol shows that (i) silicone oil and all its derivatives including amine and phenyl substituted chains produce stable emulsions, provided that oil has a polymeric character with a molecular weight exceeding about $5000\ \text{g/mol}$ (ii) polyurethane and polyester oils including their derivatives exhibit also stable water-in-oil emulsions (**fig. S3**).

These findings demonstrate the unexpected behavior of a polymeric oil when it adsorbs on the interface of a hydrophilic liquid and becomes confined in a very thin film. An inherent consequence of this weak binding of polymeric oils to the water interface, due to their slightly polar nature, is their conformational change, exposing a more hydrophobic portion of the molecule towards the bulk oil. This results in a weak adhesion between two identical interfaces and leads to a dramatic increase in the effective viscosity of the oil in the thin film as compared to its bulk value; such an effect has been

observed so far only on a solid surface (*24*, *25*). In the case of a liquid interface it must be understood as an intrinsic consequence of both adsorption and adhesion which together efficiently modify the polymer dynamics at liquid interfaces, as a direct consequence of the counterintuitive lowering of their interfacial free energy.

Conclusions

These results represent a mechanism for stabilizing water droplets in oil in the absence of surfactant. They also represent an important route to formulate materials through double emulsions made in a single step (*26*, *27*). When ϕ exceeds ϕ^*, the emulsion breaks under shear forming a double emulsion without the use of any surfactant nor any solvent whatsoever. This will have important technological applications: it enables the creation of very pure and controlled materials, particularly for polymerizable oils such as those used here.

References and Notes

1. E. Chatzigiannakis, J. Vermant, Breakup of Thin Liquid Films: From Stochastic to Deterministic. *Phys. Rev. Lett.* **125**, 158001 (2020).

2. P. Poulin, H. Stark, T. C. Lubensky, D. A. Weitz, Novel Colloidal Interactions in Anisotropic Fluids. *Science* **275**, 1770–1773 (1997).

3. J. K. Beattie, A. M. Djerdjev, The Pristine Oil/Water Interface : Surfactant-Free Hydroxide-Charged Emulsions. *Angew. Chem. Int. Ed.* **43**, 3568–3571 (2004).

4. K. Roger, B. Cabane, Why Are Hydrophobic/Water Interfaces Negatively Charged? *Angew. Chem.* **124**, 5723–5726 (2012).

5. A. Kabalnov, H. Wennerström, Macroemulsion Stability: The Oriented Wedge Theory Revisited. *Langmuir* **12**, 276–292 (1996).

6. P. Poulin, J. Bibette, Wetting of Emulsions Droplets: From Macroscopic to Colloidal Scale. *Phys. Rev. Lett.* **79**, 3290–3293 (1997).

7. P. Poulin, F. Nallet, B. Cabane, J. Bibette, Evidence for Newton Black Films between Adhesive Emulsion Droplets. *Phys. Rev. Lett.* **77**, 3248–3251 (1996).

8. P. Poulin, J. Bibette, Adhesion of Water Droplets in Organic Solvent. *Langmuir* **14**, 6341–6343 (1998).

9. A. R. Thiam, N. Bremond, J. Bibette, From Stability to Permeability of Adhesive Emulsion Bilayers. *Langmuir* **28**, 6291–6298 (2012).

10. D. Langevin, Recent Advances on Emulsion and Foam Stability. *Langmuir : the ACS journal of surfaces and colloids* **39** (2023).

11. K. Mojsiewicz-Pieńkowska, Size exclusion chromatography with evaporative light scattering detection as a method for speciation analysis of polydimethylsiloxanes. III. Identification and determination of dimeticone and simeticone in pharmaceutical formulations. *Journal of Pharmaceutical and Biomedical Analysis* **58**, 200–207 (2012).

12. B. Hogan, A. Babataheri, Y. Hwang, A. I. Barakat, J. Husson, Characterizing Cell Adhesion by Using Micropipette Aspiration. *Biophysical Journal* **109**, 209–219 (2015).

13. H. M. Princen, Geometry of clusters of strongly coagulated fluid drops and the occurence of collapsed plateau borders. *Colloids and Surfaces* **9**, 47–66 (1984).

14. M. P. Aronson, H. M. Princen, Contact angles associated with thin liquid films in emulsions. *Nature* **286**, 370–372 (1980).

15. V. Schmitt, F. Leal-Calderon, Measurement of the coalescence frequency in surfactant-stabilized concentrated emulsions. *Europhys. Lett.* **67**, 662–668 (2004).

16. K. Pays, J. Giermanska, B. Pouligny, J. Bibette, F. Leal-Calderon, Double Emulsions: A Tool for Probing Thin-Film Metastability. *Physical review letters* **87**, 178304 (2001).

17. A. B. Croll, K. Dalnoki-Veress, Hole nucleation in free-standing polymer membranes: the effects of varying molecular architecture. *Soft Matter* **6**, 5547–5553 (2010).

18. M. Ilton, C. DiMaria, K. Dalnoki-Veress, Direct Measurement of the Critical Pore Size in a Model Membrane. *Phys. Rev. Lett.* **117**, 257801 (2016).

19. B. Deminiere, A. Colin, F. Leal-Calderon, J. F. Muzy, J. Bibette, Cell Growth in a 3D Cellular System Undergoing Coalescence. *Phys. Rev. Lett.* **82**, 229–232 (1999).

20. A. E. Ismail, G. S. Grest, D. R. Heine, M. J. Stevens, M. Tsige, Interfacial Structure and Dynamics of Siloxane Systems: PDMS−Vapor and PDMS−Water. *Macromolecules* **42**, 3186–3194 (2009).

21. C. Kim, M. C. Gurau, P. S. Cremer, H. Yu, Chain Conformation of Poly(dimethyl siloxane) at the Air/Water Interface by Sum Frequency Generation. *Langmuir* **24**, 10155–10160 (2008).

22. J. P. Cohen-Addad, M. Domard, S. Boileau, Slow dynamics of entangled polydimethylsiloxane chains observed by proton transverse magnetic relaxation. *The Journal of Chemical Physics* **75**, 4107 (1998).

23. J. Götz, H. Weisser, S. Altmann, "Correlation of the Viscosity and the Molecular Weight of Silicone Oils with theT2 NMR Relaxation Times" in *Organosilicon Chemistry V*, N. Auner, J. Weis, Eds. (Wiley-VCH Verlag GmbH, Weinheim, Germany, 2003; https://onlinelibrary.wiley.com/doi/10.1002/9783527619924.ch94), pp. 584–594.

24. Z. Yang, Y. Fujii, F. K. Lee, C.-H. Lam, O. K. C. Tsui, Glass Transition Dynamics and Surface Layer Mobility in Unentangled Polystyrene Films. *Science* **328**, 1676–1679 (2010).

25. J. Klein, E. Kumacheva, Confinement-Induced Phase Transitions in Simple Liquids. *Science* **269**, 816–819 (1995).

26. J. A. Hanson, C. B. Chang, S. M. Graves, Z. Li, T. G. Mason, T. J. Deming, Nanoscale double emulsions stabilized by single-component block copolypeptides. *Nature* **455**, 85–88 (2008).

27. Z. Li, H. Liu, L. Zeng, H. Liu, S. Yang, Y. Wang, Preparation of High Internal Water-Phase Double Emulsions Stabilized by a Single Anionic Surfactant for Fabricating Interconnecting Porous Polymer Microspheres. *Langmuir* **30**, 12154–12163 (2014).

28. Y.-Q. Song, L. Venkataramanan, M. D. Hürlimann, M. Flaum, P. Frulla, C. Straley, T1–T2 Correlation Spectra Obtained Using a Fast Two-Dimensional Laplace Inversion. *Journal of Magnetic Resonance* **154**, 261–268 (2002).

29. A. Vena, S. Kolle, S. Stafslien, J. Aizenberg, P. Kim, Self-Stratifying Porous Silicones with Enhanced Liquid Infusion and Protective Skin Layer for Biofouling Prevention. *Advanced Materials Interfaces* **8**, 2000359 (2021).

30. P. Mazurek, S. Hvilsted, A. L. Skov, Green silicone elastomer obtained from a counterintuitively stable mixture of glycerol and PDMS. *Polymer* **87**, 1–7 (2016).

31. L. Champougny, E. Rio, F. Restagno, B. Scheid, The break-up of free films pulled out of a pure liquid bath. *J. Fluid Mech.* **811**, 499–524 (2017).

32. A. Sheludko, Thin liquid films. *Advances in Colloid and Interface Science* **1**, 391–464 (1967).

33. A. Vrij, Possible mechanism for the spontaneous rupture of thin, free liquid films. *Discuss. Faraday Soc.* **42**, 23–33 (1966).

34. J. N. Israelachvili, P. M. McGuiggan, Forces Between Surfaces in Liquids. *Science* **241**, 795–800 (1988).

35. A. Vrij, J. Th. G. Overbeek, Rupture of thin liquid films due to spontaneous fluctuations in thickness. *J. Am. Chem. Soc.* **90**, 3074–3078 (1968).

Acknowledgements

Fundings

Calyxia (CN)

Capsum

Institut Pierre-Gilles de Gennes (Équipement d'Excellence, "Investissements d'avenir," program ANR-10- EQPX-34)

National Science Foundation (NSF) through the Harvard Materials Research Science and Engineering Center (MRSEC, DMR-2011754).

Author contributions

Conceptualization: CN, DD, JW, NB, JBa, JBi

Methodology: CN, NB, JBa, JBi

Investigation: CN, AC, YS, AS

Visualization: CN, AC, YS, NB, JBa, DAW, JBi

Writing – original draft: CN, JBa, JBi

Writing – review & editing: CN, NB, JBa, DAW, JBi,

Competing interests

CN, DD, JBa and JBi hold patents related to this work (European unexamined patent application EP22305808 and French unexamined patent application FR2306227).

DAW and JBi are co-founders and shareholders of Calyxia.

DAW and JBi have advisory activities for Calyxia.

Data and materials availability:

All data are available in the main text or the supplementary materials.

List of supplementary materials

Materials and Methods

Supplementary Text

Fig. S1, S2, S3

Movie S1

References (*28*–*35*)

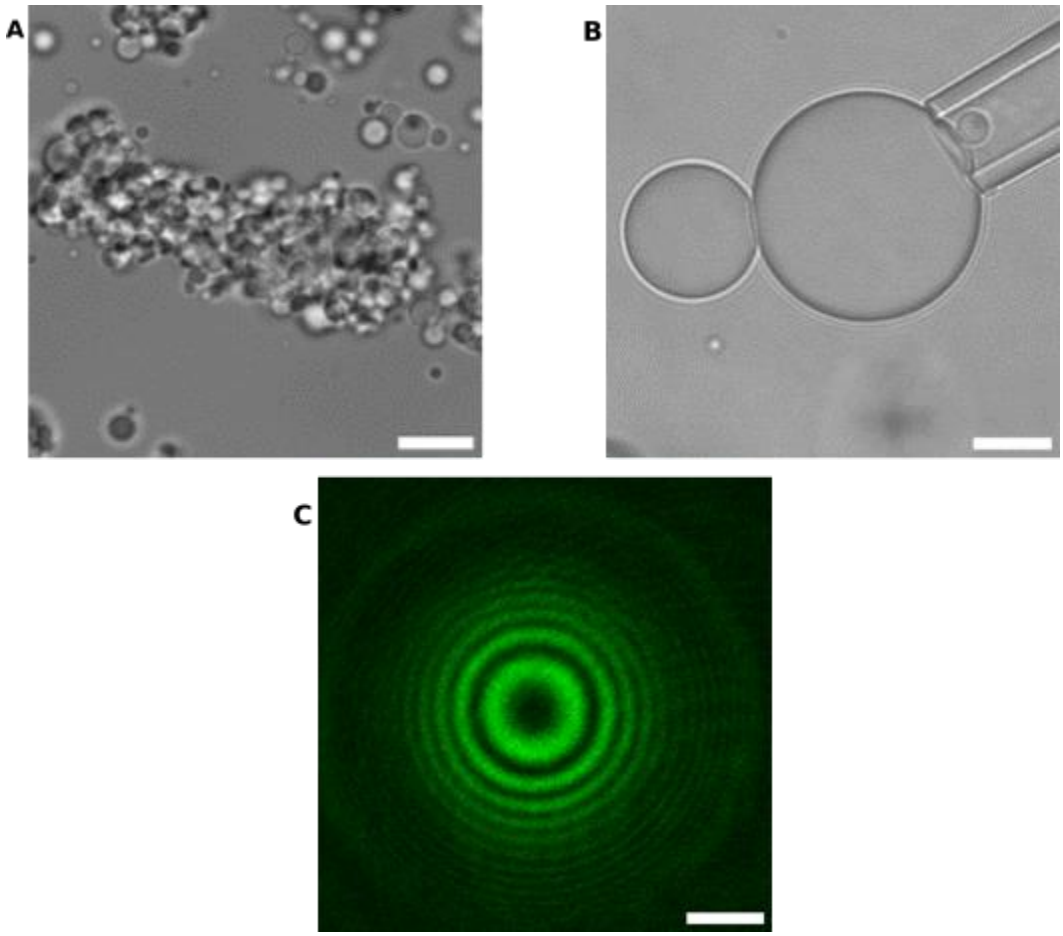

Fig. 1. **Adhesion in glycerol/PDMS emulsion.** (**A**) Large stable and compact clusters of droplets: evidence of adhesion between droplets. Scale bar is 10 µm. (**B**) Capture of a doublet comprised of two adhesive droplets using a micropipette aspiration. Scale bar is 10 µm. (**C**) Transverse imaging of the oil film separating the adhesive droplets: the thin black film (central dark fringe) gives the size of the adhesive patch formed between two droplets of about 50 µm diameter. Scale bar is 2 µm.

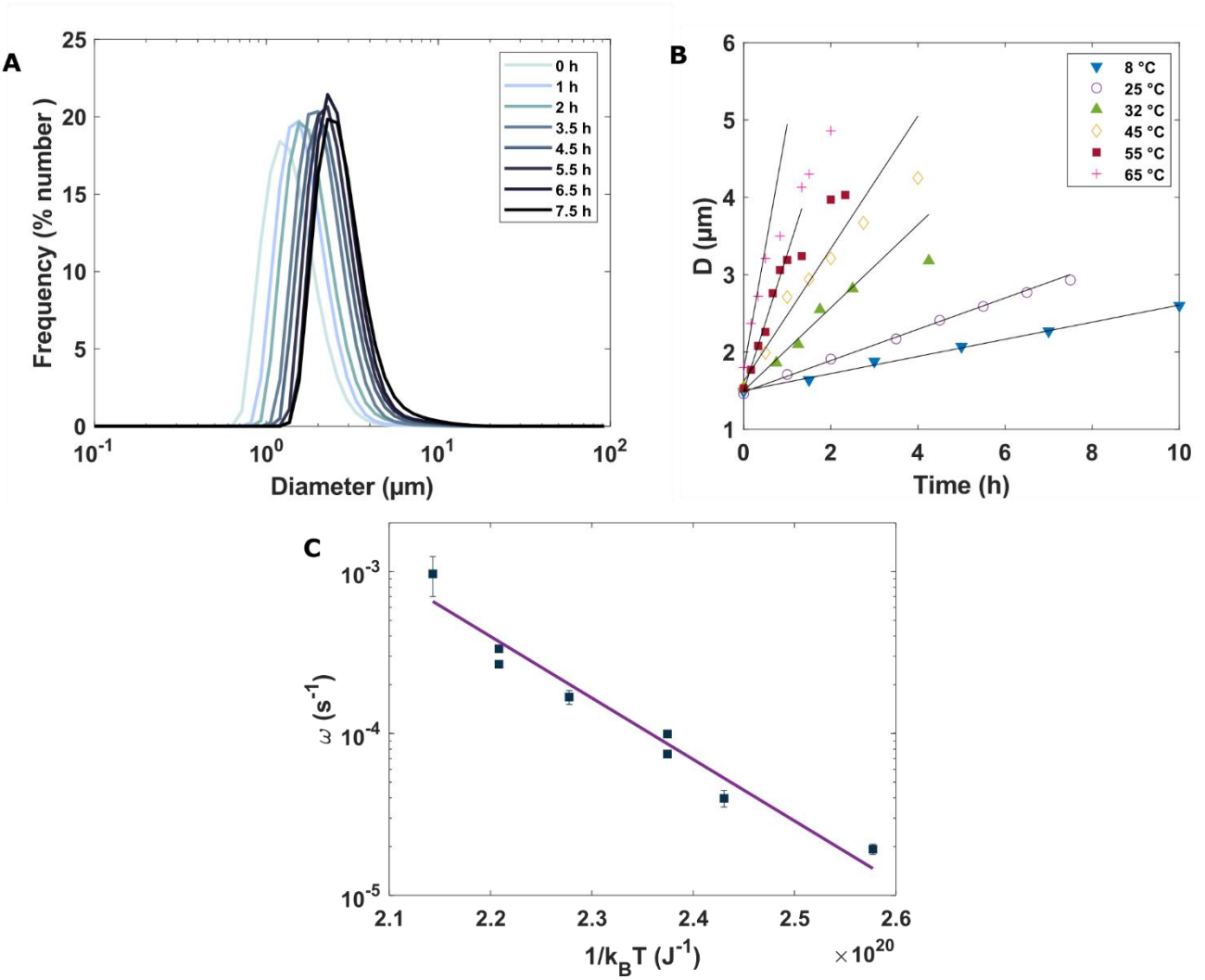

Fig. 2. Coarsening of a concentrated glycerol/PDMS oil emulsion. (**A**) Droplet size distribution of a glycerol in PDMS oil emulsion at a volume fraction $\phi = 76\%$, as a function of time upon storage at 25°C. (**B**) Droplet mean diameter as a function of time under different storage temperatures. (**C**) Arrhenius plot: ω as a function of $1/k_BT$ (error bars are specified for N=3).

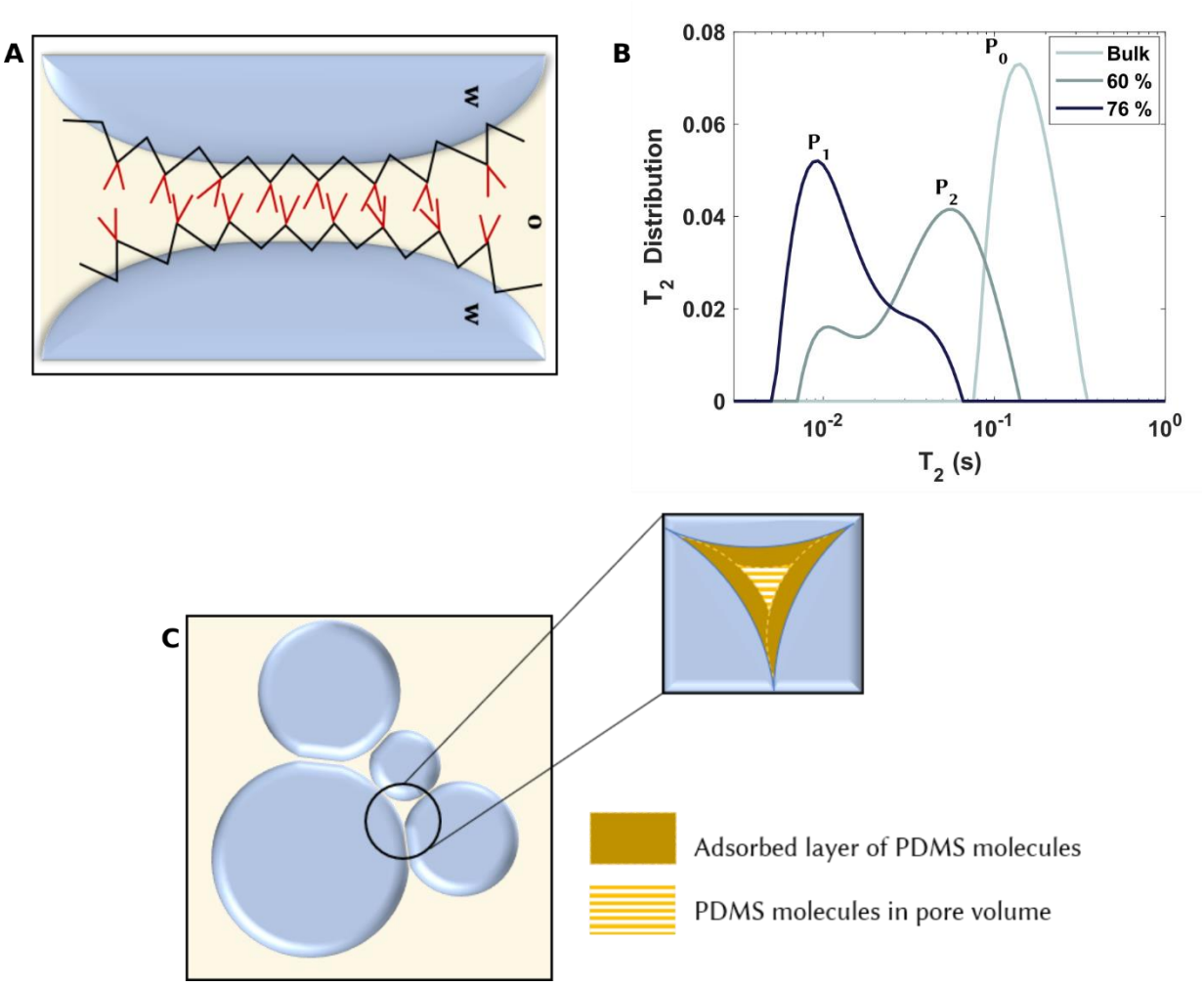

Fig. 3. Specific adsorption of oil molecules at the interface. (**A**) Schematic representation of the interaction mechanism between PDMS oil/glycerol interfaces: the hydrophobic moieties of the oil (methyl group in red) specifically adhere while the hydrophilic parts of the backbone composed of oxygen atoms are preferentially adsorbed on the glycerol surface, this may account for the attraction between the droplets. (**B**) Plot of T_2 relaxation time distribution as a function of time for PDMS used as the continuous phase of a glycerol/PDMS oil emulsion compared to its bulk value. The bimodal T_2 distribution indicates that within the emulsion, PDMS molecules are of two types: one is confined in the thin film, the other is trapped in the Plateau borders of the emulsion. (**C**) Schematic representation of the pore surrounded by droplets, the so-called Plateau border: the PDMS contained in Plateau borders is either located in the adsorbed layer or confined in this pore volume.

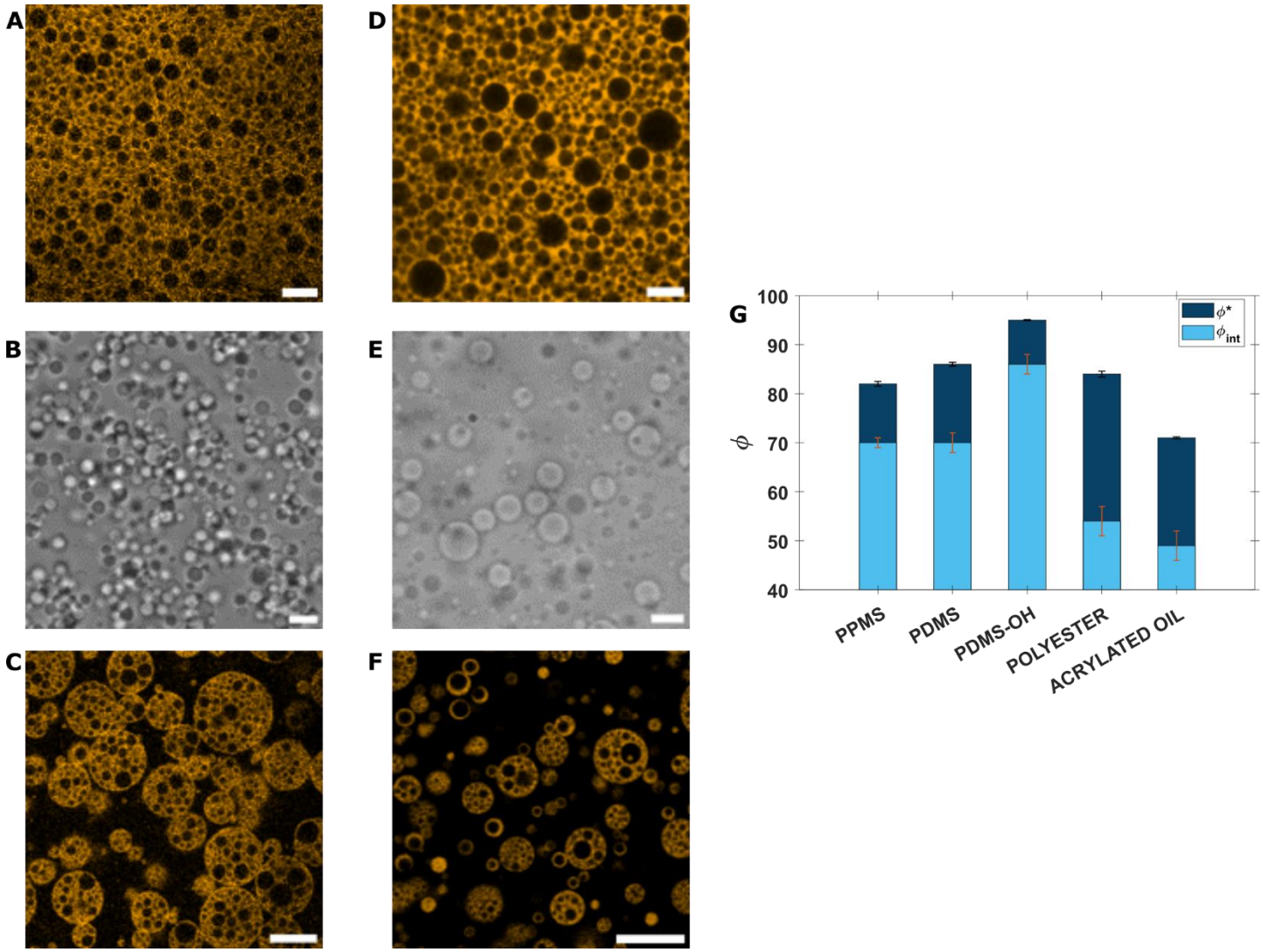

Fig. 4. Emulsions formed with different oils without surfactants. (**A**) A stable emulsion of glycerol in hydroxy-terminated PDMS oil (dyed orange) can be prepared at higher ϕ of 80%. Scale bar is 5 µm. (**B**) Microscopic picture of a diluted glycerol in hydroxy-terminated PDMS oil emulsion: evidence for compact connected clusters. Scale bar is 5 µm. (**C**) Double emulsion obtained with the hydroxy-terminated PDMS oil after phase inversion at $\phi^* = 95\%$. Scale bar is 10 µm. (**D**) A stable emulsion of glycerol in acrylated vegatable oil (dyed orange) can be prepared at ϕ of 70%. Scale bar is 5 µm. (**E**) Adhesion is also evidenced in a diluted glycerol in acrylated vegetable oil emulsion. Scale bar is 5 µm. (**F**) Double emulsion obtained with the acrylated vegetable oil after phase inversion at $\phi^* = 71\%$. Globules are less concentrated in internal phase as $\phi_{int} = 49\%$. Scale bar is 10 µm. (**G**) Critical volume fraction ϕ^* at which inversion takes place and internal fraction of glycerol within double globule ϕ_{int} ; both fractions depend on the chosen water/oil couple only (N=3, Methods 5).

Science
AAAS

Supplementary Materials for

Thin adhesive oil films lead to anomalously stable mixtures of water in oil

Authors: Claire Nannette, Jean Baudry, Anqi Chen, Yiqiao Song, Abdulwahed Shglabow, Nicolas Bremond, Damien Démoulin, Jamie Walters, David A. Weitz, Jérôme Bibette

Corresponding author: jerome.bibette@espci.fr

The PDF file includes:

- Materials and Methods
- Supplementary Text
- Figs. S1 to S3

Other Supplementary Materials for this manuscript include the following:

- Movie S1

Materials and Methods

Materials

The following chemicals were purchased from Sigma-Aldrich and were used as received: glycerol (G7757, viscosity ~840 mPa.s) PDMS (polydimethylsiloxane) oil methyl-terminated (378399, viscosity~ 1,000 mPa.s and 378372, viscosity ~350 mPa.s), PDMS oil hydroxy-terminated (481963, viscosity ~750 mPa.s), PPMS (polyphenylmethylsiloxane) oil (10842, AP 1000 viscosity ~1,000 mPa.s), hexadecane ($H6703$), anisole (123226), Nile Red (72485), PVA (polyvinyl alcohol, $363170, \mathrm{M_w} \sim 13{,}000 - 23{,}000\ \mathrm{g/mol}, 87 - 89\%$ hydrolyzed). Polyester (Priolube 1847) was purchased from Croda. Soybean epoxided acrylated oil (Genomer 2312) was purchased from Rahn. Silube J208-812 was received from Siltech. The acrylated oil was diluted at 83% in anisole in order to lower its viscosity.

Interfacial tension measurements were made using the pendant drop method (Kruss DSA30 tensiometer). The glycerol/methyl terminated PDMS oil interfacial tension was measured to be $25\ \mathrm{mN/m}$.

Methods 1: Emulsion fabrication

For emulsion fabrication, glassware was first cleaned using detergent and then rinsed thoroughly using ethanol and DI water (Milli-Q water, Millipore).

To formulate the emulsions, the aqueous and oil phases were sheared using an overhead stirrer (IKA Eurostar 40) equipped with a 4-bladed helix propeller (IKA, R 1342, 50 mm diameter) rotating at 1000 RPM. Emulsions were prepared in a glass beaker (VWR, 213-1172, 55 mm internal diameter) immersed in a water bath to maintain a temperature around $25℃$. The aqueous phase was added dropwise into the oil phase using a syringe pump (Harvard Apparatus PHD Ultra) set at 25 mL/hr to concentrate the emulsion until desired internal phase volume fraction ϕ was reached. The typical total volume of the prepared emulsions was about 10 mL. Nile Red was mixed with the oil phase for fluorescence microscopy observations.

Bright-field microscopy images of the emulsions were obtained using a Nikon Eclipse E600 microscope equipped with a Hamamatsu Orca-R2 camera. Confocal laser scanning microscopy images were obtained using a Nikon Eclipse Ti-E microscope equipped with a Nikon D-Eclipse C1si controller, a 540 nm laser and an appropriate TRITC filter.

Methods 2: Micropipette aspiration

A crude emulsion was prepared by gently mixing glycerol in methyl terminated PDMS oil (350 mPa.s). The emulsion was then further diluted at $\phi \approx 10\%$ and introduced inside an observation chamber made with two coverslips (VWR, 16004-302) sandwiching a 1 mm silicone spacer (Invitrogen, P24744) which is cut on one side to allow the insertion of the micropipette. A glass capillary (World Precision Instrument 1B100-6, outer diameter 1 mm, inner diameter 0.58 mm) was pulled using a Micropipette Puller (P97, Sutter Instrument Company) and cut into a 10 μm tip using a microforge (MF830,

Narishige). The capillary was filled with the oil phase and connected to a pressure controller system with a negative pressure range of $0 - \sim 25$ mbar (Fluigent). A duet of adhesive droplets was then captured using the micropipette.

Methods 3: Contact angle determination

Contact angle determination was made through imaging of the oil film separating two adhesive droplets of diameter D_1 and D_2 captured following the micropipette aspiration technique presented in Methods 2. The oil film was imaged in the transverse direction using a confocal microscope (Leica SP5) equipped with a 488 nm laser and a RT 30/70 filter to obtain the interference profile of the thin film. The dark central fringe corresponds to the adhesive patch of diameter a. Measurement of a was performed under ImageJ image analysis software using an intensity profile. The contact angle can then be determined from the following equation (*13*): $2\theta = \sin^{-1}\left(\frac{a}{D_1}\right) + \sin^{-1}\left(\frac{a}{D_2}\right)$. For such small contact angles, this approach is much more precise than a direct measurement made by imaging a profile view of two drops where the adhesive patch is perpendicular to the plane of focus.

Methods 4: Droplet size distribution

Droplet size distributions of the emulsion were measured through static light scattering (SLS) using a Malvern Mastersizer 3000. A few µL of emulsions was diluted in hexadecane containing 1% Silube J208-812 as surfactant to perform the measurement.

Temperature-dependent measurements were obtained by storing the prepared emulsion at a given temperature in an oven. At regular intervals, a sample was taken and the droplet size distribution measured. For each distribution, the mean diameter D was determined from the first moment of the size distribution function $D[1:0] = \frac{\sum n_i D_i}{\sum n_i}$. For each temperature, the experiment was performed twice.

Methods 5: ^{1}H NMR relaxometry

^{1}H NMR (Nuclear Magnetic Resonance) spectroscopy was performed on a 600 MHz Bruker Avance III HD spectrometer (Bruker Biospin) at Martinos Center for Biomedical Imaging, Massachusetts General Hospital. T_2 relaxation was measured by CPMG (Carr-Purcell-Meiboom-Gill) pulse sequence with an echo time of 1 ms. Integration over 1 kHz around the PDMS signal was performed to obtain the PDMS signals for all echo decay times from 1 to 200 ms. The signal was further processed by the Fast Laplace Inversion algorithm to obtain the T_2 distributions (*28*).

Methods 6: ϕ_{int} measurement

Emulsion samples were prepared following the procedure described in Method 1. At ϕ^*, when phase inversion occurred, $10-50$ µL of a 20% PVA solution was added to the inverted emulsion in order to stabilize the globules and enable further processing. Around 400 µL of emulsion was then introduced into a polyamide centrifugation tube (LUM GmbH, 2 mm thick). The emulsion was centrifuged (LumiFuge™) for 30 min at 2300 g (4000 RPM). This step allowed all globules to coalesce under compression without altering the stability of the internal emulsion. After centrifugation, the sample turned into a cream layer containing the internal W/O emulsion on top of the extracted external water phase. Measurement of the cream layer volume fraction ϕ_{cream} thanks to the optical analysis provided by the SEPView software helped deducing ϕ_{int}, as $\phi_{\text{int}} = 1 - \frac{1-\phi^*}{\phi_{\text{cream}}}$. Each emulsion was prepared three times for reproducibility testing.

Supplementary Text

PDMS oil purification protocol

Concentrated water-in-PDMS oil emulsions have been previously described in the literature (*29*, *30*). Although these emulsions were also containing cross linkers they were not supposed to contain surfactant. Some authors did attribute the surprising persistence of these emulsions before being polymerized to a preferential adsorption of short-chain PDMS molecules acting as surfactants. In order to investigate the role of these molecules, we performed a fractionation protocol of PDMS oil (*31*). 20 mL of PDMS oil was vigorously mixed with 60 mL of acetone in a separating funnel. After complete phase separation, the PDMS fraction was recovered and placed first in an oven at 65°C for 24h and under vacuum for another 24h for complete removal of residual acetone. Fractionated PDMS oil was then used for emulsification. No significant difference was noticed compared to a non-fractionated sample.

Comparison to other measurements of the adhesive energy

The value measured for the adhesive energy, ε, for the surfactant free glycerol-in-PDMS emulsion can be compared to that measured with the same experimental method for a surfactant-stabilized inverse emulsion, consisting or water drops in dodecane, stabilized by sorbitan monoleate (SPAN 80). By adding 25% by volume silicone oil to dodecane, the solubility of the SPAN 80 is reduced, inducing an attractive interaction between the water droplets. When the concentration of the poor solvent, silicone oil, is below the threshold concentration for surfactant precipitation in the dodecane-silicone-oil mixture, the attractive interaction is weak and is measured to be $\varepsilon = 2 \times 10^{-2}$ mJ/m^2 (*8*). This value is nearly identical to that measured here for the glycerol-in-PDMS emulsion, where we find $\varepsilon = 3 \times 10^{-2}$ mJ/m^2. Interestingly, in both cases, the adhesive energy originates from similar mechanisms. In the case of the surfactant free emulsion, it is an intrinsic consequence of the oil adsorption, whereas in the case of the surfactant stabilized emulsion, it is a consequence of the quality of the solvent that is modified by adding a fourth component. This adhesive interaction induces similar consequences in both systems: the gelation of the droplet dispersion into large and dense clusters that can percolate across the whole sample.

Capillary model for nucleation and growth

In the paper, we consider a thin film of constant thickness, and use the capillary model to determine the nucleation and growth of a hole that leads to coalescence of the droplets. The thickness of the thin film is set by the wetting of the interfaces. According to the capillary model, the energy related to the nucleation and growth of a hole of radius r within a liquid film writes $E(r) = -2\pi r^2\gamma + 2\pi r\Gamma$, where γ is the surface tension and Γ is the line tension. The first term of this equation accounts for the decrease of surface area within the film while the second term accounts for all contributions associated with the inherent high curvature at the edge of the hole. Considering these two opposite contributions, there must exist a critical radius r^* for which the growth of the pore is energetically favored. For $r = r^*$, the value of the resulting energy is expressed as an activation energy E_a. By taking the derivative, one can get $\frac{dE(r)}{dr}_{|r^*} = -4\pi r^*\gamma + 2\pi\Gamma = 0$. An expression of r^* can thus be directly decuced $r^* = \frac{\Gamma}{2\gamma}$. Finally, the expression of E_a which equals $E(r^*)$ can only be written as a function of r^* and γ. This leads to $r^* = \left(\frac{E_a}{2\pi\gamma}\right)^{1/2}$. This capillary model is appropriate for the conditions of a metastable interface of constant thickness, as is the case in these experiments.

Thin film instability

An alternative approach to treat the instability of a thin film is to consider the effect of thermally induced capillary waves on each interface in the presence of an attractive interaction due to van der Waals forces, and to calculate the time it takes for the interfaces to touch leading to coalescence.

We evaluate an effective viscosity of PDMS in the adhesive patch by using the timescale of the film rupture, initially at rest, due to the amplification of thermal thickness fluctuations by van der Waals attraction (*32*). The free energy cost due to interfacial tension imposes a critical wavelength λ_c of such fluctuations below which they are not amplified (*33*)

$$\lambda_c = \left(\frac{-2\pi^2\gamma}{\left(d^2E/dh^2\right)_0}\right)^{1/2} \quad (1)$$

where γ is the interfacial tension and $E(h)$ is the free energy of interaction per unit surface which is a function of the film thickness h. When repulsive forces are small compared to attractive ones, one can consider only van der Waals attraction,

$$E(h) = -\frac{A}{12\pi h^2} \quad (2)$$

where A is the Hamaker constant which can be approximated by

$$A = \frac{3}{4}kT\left(\frac{\varepsilon_d - \varepsilon_c}{\varepsilon_d + \varepsilon_c}\right)^2 + \frac{3h\nu_e}{16\sqrt{2}}\frac{\left(n_d^2 - n_c^2\right)^2}{\left(n_d^2 + n_c^2\right)^{3/2}} \quad (3)$$

with ε_d, ε_c, n_d and n_c being the static dielectric constant and the refractive index in the visible of the dispersed phase and the continuous phase, respectively, and ν_e is the main electronic absorption frequency in the UV (*34*). For the system

493 composed of glycerol and PDMS oil, the theoretical estimation of A is equal to 3.8×10^{-21} J. The critical wavelength is
494 then

496 $$\lambda_c = h_0^2 \left(\frac{4\pi^3\gamma}{A}\right)^{1/2} \quad (4)$$

495

497 where h_0 is the average film thickness.

498 The growth kinetics of the thickness modulations depends on viscous resistance of the liquid flow which is mainly related
499 to the viscosity η of the liquid in the film. A perturbation with a wavelength λ close to λ_c has a low growth rate σ since the
500 restoring force due to the interfacial tension is high. The capillary pressure is proportional to the curvature which varies as
501 $1/\lambda^2$ and acts against the flow from the node to the crest of the thickness modulations (**fig. S2**). A perturbation with a long
502 wavelength also has a low growth rate because fluid has to move over a long distance. Therefore, there exists a wavelength
503 λ_m leading to a maximum growth rate $\sigma_m = 1/\tau_m$ which can be deduced by a linear stability analysis (*35*) leading to

504 $$\lambda_m = \sqrt{2}\lambda_c \quad (5)$$

505 and

506 $$\tau_m = \frac{96\pi^2\gamma\eta h_0^5}{A^2} \quad (6)$$

507 A small perturbation δh of the thickness will then grow exponentially with time with a characteristic time τ_m, i.e. $h = h_0 +$
508 $\delta h\, e^{t/\tau_m} \sin 2\pi x/\lambda$ with x being a coordinate parallel to the average film interface (**fig. S2**).

509 The average time of film breakup t_b can be estimated by assuming that rupture occurs when the mean square of the thickness
510 deviation from the average thickness, i.e. $\overline{h^2 - h_0^2}$ is of the order of h_0^2. By solely considering the most amplified mode and
511 using the principle of equipartition, the following equation is obtained (*33*)

512 $$h_0^2 \approx \frac{kT}{2\gamma\pi^{1/2}} \frac{e^{2t_b/\tau_m}}{(2t_b/\tau_m)^{1/2}} \quad (7)$$

513 The solution of eq. (7) then gives a linear relationship between t_b and τ_m, $t_b = f(h_0, \gamma)\tau_m$. Using eq. (6), the viscosity of
514 the liquid in the liquid film is

515 $$\eta = \frac{A^2 t_b}{96\pi^2\gamma h_0^5 f} \quad (8)$$

516 We assume here that adhesion leads to the formation of a thin film that is twice the distance from the PDMS-water interface
517 where the order parameter of methyl group of PMDS determined by molecular dynamics simulations is higher than the
518 average one of the bulk phase (*20*), which is about 1 nm. An estimate for the adhesive film thickness h_0 is thus 2 nm. If we

assume that t_b corresponds to the characteristic time of let size evolution $1/\omega$ (**Fig. 2**), which is about 4.3 h at 25°C, we can estimate a corresponding viscosity of the order of 10^5 Pa. s where f evaluated from eq. (7) is about 2.6.

Rationalizing the observed long lifetime of glycerol in PDMS emulsions by using thin film instability mechanism also requires a large increase of the oil viscosity in the adhesive patch as compared to its bulk value. However, this model does not take into account the wetting of the interfaces which leads to an equilibrium thickness set by a short range repulsion, and intrinsically results in the existence of an activation energy. For this reason, the nucleation model is a better description of the behavior.

Other contributions to the adhesion observed in emulsions: double layer effects and van der Waals interactions

Since there is no charge in the system, there are no double layer effects. In order to confirm this, we have added salt into the dispersed phase up to $0.5\ \mathrm{mol/L}$ and verify that the entire phenomenology was conserved. By contrast van der Waals interactions should be present and could also contribute to the overall adhesion that we observe. However, when we use different molecular weight oils of the same nature (PDMS oil for example) for which the magnitude of van der Waals interactions should be the same, we observe a gradual decrease of the adhesion when the molecular weight decreases, until it disappears at which point the droplets are no longer stable. These results suggest that van der Waals interactions are not the dominant contribution in the formation of this adhesive patch although they are important in driving the growth of the hole for droplets to coalesce.

Decay of P_1 peak intensity in the NMR relaxation experiment

The contribution to the P_1 peak is primarily the oil in the thin adhesive film located between neighboring droplets. At volume fraction of 60% the droplets are at roughly random close packing in which case the average number of nearest neighbors is 6. By contrast at volume fraction of 76% the packing is much denser and roughly hexagonal which increases the average number of nearest neighbors to about 10, which is increased even further by polydispersity. Accordingly, the number of PDMS molecules probed through the NMR relaxometry strongly rises. Hence the change in the peak amplitude from 76% to 60% volume fraction.

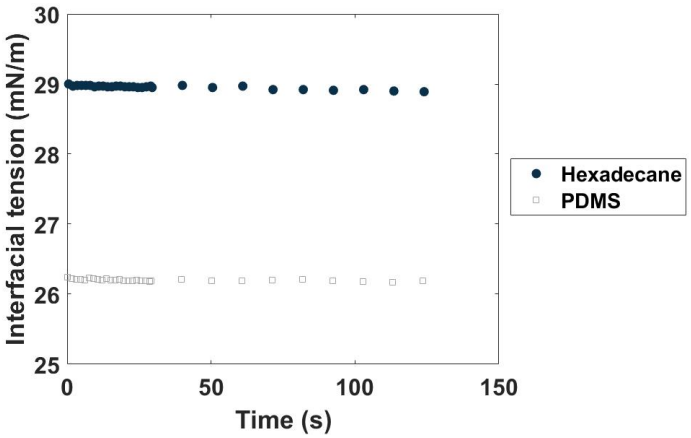

fig. S1. Interfacial tension evolution over time of a glycerol droplet in oil. PDMS oil was fractionated prior to this measurement. The interfacial tension (IFT) remains stable over time, confirming the purity of the oil.

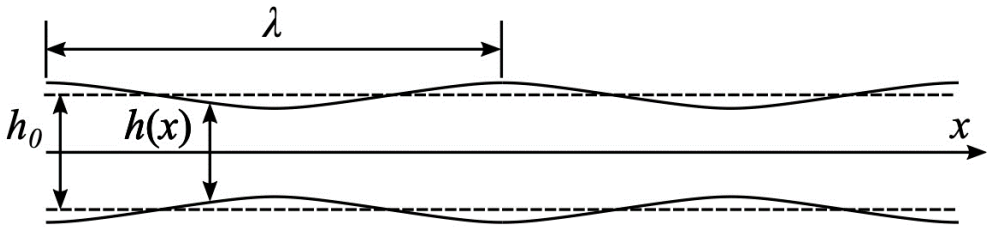

fig. S2. Sinusoidal modulation with a wavelength λ of the thickness of a thin liquid film. The film has an average thickness h_0.

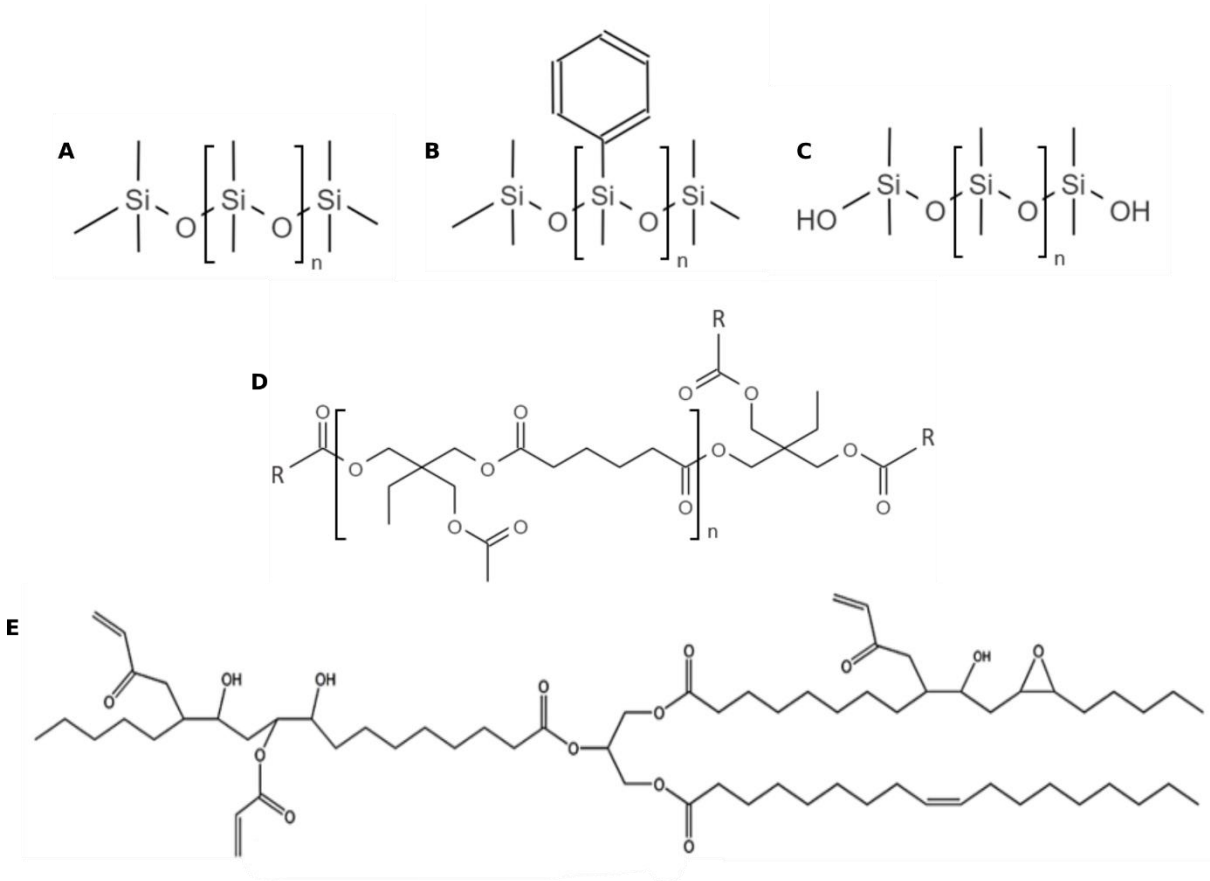

fig. S3. Examples of oil polymeric backbones. (**A**)**,** PDMS methyl terminated. (**B**), PPMS. (**C**)**,** PDMS hydroxy terminated. (**D**)**,** Polyester. (**E**)**,** Acrylated soybean oil

Movie S1. Coalescence event in a glycerol-in-PDMS emulsion. A glycerol-in-PDMS emulsion is obtained by dispersing about 1% by volume of glycerol into PDMS oil ($\eta = 350$ cp). We deposit $20\ \mu L$ of this emulsion on a glass slide and directly observe with a microscope (X10) at $T = 60°C$. The emulsion evolution is recorded for a duration of 200 s with a frame captured every 2 s. The number of doublets within the recorded zone is evaluated to be around 100. During the entire recording period the number of coalescence events which are observed within this zone is about 5, which suggests a coalescence frequency per doublet of about $2.5\ 10^{-4}s^{-1}$. This is in agreement with the value of $\omega = 5\ 10^{-4}s^{-1}$ deduced from the coarsening of a dense emulsion at $60°C$. In this movie, we focus on just one of these events which occurs between the frames at 32 and 34 s: Two adhesive droplets of about 10 microns in diameter within a linear triplet suddenly merge as a result of coalescence. The scale bar is $10\ \mu m$.